



CLOSED-ORBIT CORRECTION FOR THE NAL MAIN RING

J. A. MacLachlan

January 1973

Introduction

The failure of the high-energy equilibrium orbit to pass through the centers of all the quadrupoles is due primarily to transverse errors in the position of the quadrupoles. Vertical-orbit distortion is also caused by roll of bending magnets about their longitudinal axis. If the radio frequency and bending magnet excitation do not track perfectly the horizontal closed orbit contains an additive part proportional to the off-momentum orbit function x_p , which must be subtracted out to isolate that part of the magnetic field error caused by misalignment. From measurements of the closed orbit one can calculate compensatory displacements of the quadrupoles to reduce the distortion and thereby increase the usable aperture. At the injection energy of 8 GeV the remanent field errors of the bending magnets make a large contribution to the closed-orbit distortion. The low-field orbit is corrected by dc correction dipoles located near the quadrupole positions. This paper describes the correction strategy we use, the relative merits of alternative mathematical tactics, and operational experience.



The emphasis is on the high-field case for which the practical difficulty in executing the corrections, i.e. in moving ring quadrupoles, places a premium on adequate correction from the fewest moves.

Relevant Features of the NAL Main Ring

The NAL 400-GeV synchrotron has a 96-cell separated function FODO lattice containing 240 quadrupole magnets. The betatron oscillation numbers are, horizontally, $\nu_x = 20.3$ and, vertically, $\nu_y = 20.2$. In the normal lattice cells, i.e. those without a long straight insertion, there is a sensor attached to the downstream end of each quadrupole to measure the beam position in the plane for which the quadrupole is focusing. In the six cells with long straight insertions there are also two matching doublets of four quads each. In the centers of each doublet there is a combined sensor for both planes. There are thus 108 sensors for each plane or about five per betatron wavelength.

The sensors (Fig. 1) are split parallel plate induction electrodes connected by coaxial cables to the nearest of the twenty-four service buildings distributed around the ring. In bench tests these detectors have demonstrated close conformity with the ideal linear response

$$x = \frac{w}{2} \frac{V_A - V_B}{V_A + V_B}, \quad (1)$$

where V_A and V_B are the voltages detected on plates A and B, respectively, and w and x are shown in Fig. 1. The beam-position system as a whole, however, does not realize the full detector

performance primarily because of variability in the cable losses from detector to service building. Because the displacement is measured by a voltage ratio the absolute losses are not important, but with attenuation on the longer runs as great as 80%, a small difference between the two cables from the same detector can introduce significant error. Because of continuing activities in the tunnel such differences may fluctuate in time and a scattered 1 to 2% of the detectors may be completely inoperative. The important measure of the system performance is thus the empirical "rms" uncertainty of about .05" vertically and .1" horizontally established by repeated cable measurements and closed-orbit determinations.

Another result of ongoing activities in the tunnel is that the closed-orbit distortion can show significant changes in a few days. Besides installation of new equipment and an occasional quadrupole replacement we still have some differential settling of the tunnel to contend with. Therefore, we have not sought a single-step solution for closed-orbit distortion but instead a tolerable method to cope with frequent approximate adjustments. Our basic strategy has been to seek a minimum number of quadrupoles which will reduce the maximum orbit distortion by a factor of two to three. We observe as constraints that the vertical closed-orbit distortion be less than 1/8" at the extraction septum, that displacements not be so large as to require realignment of bending magnets or other devices from their surveyed positions, and that available quadrupole travel not be exceeded. After each set of moves the remeasured orbit is used to calculate the next step

of correction. We have not been able to establish completely fixed computational tactics which implement this strategy successfully for all our data. Experience has shown, however, that a rather limited set of analytical tools suffices and that it is reasonably straightforward to select the proper combination for a specific set of data.

Computational Techniques

The high-field closed-orbit distortion x_i measured at the i th sensor is a sum of contributions proportional to quadrupole displacements δ_j :

$$x_i = \sum_j a_{ij} \delta_j. \quad (2)$$

Because the betatron phase advance through a quadrupole is nearly zero, the formula derived from a δ -function kick,

$$a_{ij} = \frac{\sqrt{\beta_i \beta_j} K_j}{2 \sin \pi \nu} \cos(\mu_i - \mu_j - \pi \nu) \quad (3)$$

is accurate to better than 1%. In this formula, β_i and β_j are the Courant-Snyder⁽¹⁾ amplitude functions at the sensor and displaced quadrupole, respectively, μ_i and μ_j are the corresponding betatron phases, ν is the betatron oscillation number, and K_j is the strength of the j th quad.

A. Least Squares Solution

Because of the uncertainty in the data, x_i , and the desire to keep the number of correcting moves much smaller than the number of sensors, it is natural to regard Eq. (2) as the equation of condition on the fitting of the closed orbit by members of the

family of functions generated by displacing each of the quadrupoles unit amount. The coefficient a_{ij} is the value of the j th member of this family at μ_i . Although the most direct approach to the stated objective of minimizing the maximum-orbit distortion would appear to be fitting according to a minimax criterion, numerical experiments have shown that such solutions vary markedly with the addition of small amounts of random error to the orbit data and that a single bad sensor reading can dominate the fit. We therefore rely on the familiar least squares principle. Extra weight placed on sensors showing maximum readings can have the practical effect of the minimax technique along with similar disadvantages. However, with least squares there is a continuous range of weights to choose from and one can check the sensitivity of the solution to a change in weights. The normal equations with arbitrary weights are conveniently expressed in the matrix form

$$A^T D A \Delta = A^T D X \quad (4)$$

where X is the column vector of closed-orbit measurements, A is the matrix of the coefficients a_{ij} , Δ is the solution vector of fitted δ_j , and D is the diagonal matrix of the weights squared. The basis set is far from orthogonal, but even in hundredfold fits there is generally no difficulty in solving the normal equations to useful precision.

B. Harmonic Analysis

The circular harmonics are an orthogonal basis with special usefulness in interpretation of the data. By expressing the closed-orbit distortion x as

$$x = \beta^{1/2} \sum_{n=-\infty}^{\infty} c_n e^{in\phi} \quad (5)$$

where β is the Courant Snyder β function and

$$0 \leq \phi = \int \frac{ds}{v\beta} \leq 2\pi \quad (6)$$

one can derive from the differential equation for the closed orbit an expression for the field error

$$\frac{\Delta B}{B\rho} = \beta^{-3/2} \sum_{n=-\infty}^{\infty} \frac{v^2 - n^2}{v^2} c_n e^{in\phi}. \quad (7)$$

Although ΔB is treated formally like x , a continuous variable, we have position values sufficient to carry the sums only through about fiftieth order. The spatial resolution in a plot of ΔB is therefore inadequate to reflect accurately the errors from individual quadrupoles. However, a single displaced quadrupole shows up as a ΔB symmetrical about the quadrupole location. Fig. 2 shows the orbit distortion $\beta^{-1/2}x$, the thirtieth order Fourier fit, and the corresponding $\beta^{3/2}\Delta B/B\rho$ from Eq. 7 for a single displaced quad. One can see that, although the closed-orbit cusp is not well fitted, the phase change is well localized. In the absence of other displaced quadrupoles nearby, any of the three curves clearly indicates the location of the displaced magnet.

1. High Field Orbit

One way to use Eq. 7 is as the solution. As suggested by Lambertson and Laslett⁽²⁾ one should ignore the highest harmonics, which are particularly influenced by sensor errors, and the lowest, which may require substantial smooth deformations of the machine

while producing negligible effect on the orbit distortion. Although these authors use the eigenvectors of $A^T A$ as a basis, their analysis is quite similar to the harmonic analysis and reduces to it almost exactly for the case with independently-positioned quadrupoles when only the focusing quadrupoles in normal cells are considered. When one treats both focusing and defocusing quads including those in the long straight sections the two analyses are no longer the same, but the qualitative conclusions of Lambertson and Laslett still apply. Fig. 2 demonstrates for a single displaced quad that even though the calculated ΔB is not strictly localized, the corrected orbit is satisfactory. This solution is not generally useful to us in the high field case because nearly every quadrupole must be moved. However, a few quads at the locations of ΔB peaks will often give a good least squares fit using Eq. 4.

2. Low-Field Orbit

It is for the low-field orbit that we have made the most regular use of the harmonic correction technique.⁽³⁾ Because the ΔB arises mostly from remanent field it changes from day to day according to changes in magnet excitation cycle and magnet changes. Also, the injection steering is not always the same. Therefore, to maximize coasting beam at injection the operators make a trial and error search in amplitude and phase for the twentieth and a few neighboring harmonics. This can be done with noclosed-orbit measurement and computer support from only the control computer. These harmonic settings are added to any

that are needed for injection steering or quadrupole displacement correction.

3. Data Smoothing

One important application of the harmonic analysis in the high-field case is to reduce the sensitivity of the calculation to sensor errors. Eq. 7 shows that only harmonics in ΔB near the twentieth produce significant orbit distortion and therefore significant components at high harmonics, say greater than the thirtieth, are due primarily to sensor error. Random error in the orbit measurements will contribute roughly equal amplitudes in all orders and the effect of these errors can be partly removed by replacing $\beta^{-1/2}x$ by its sum to thirtieth order. Data points with very large residuals are probably in error; a better answer may be obtained by ignoring them entirely.

D. Search Algorithm

All that is needed to get the solution according to Eq. (4) is a way to choose a set of quads to move for the correction. We have found most generally useful a systematic trial and error search like that used at the CERN ISR.⁽⁴⁾ The n th step of this iterative cycle fits the closed orbit with every n -fold combination of quads consisting of the $n-1$ selected in the prior steps and one of those not selected. The n -tuple which reduces the rms orbit distortion by the largest amount is the optimum set for this step. Thus, the first step, for example, finds the single quad which generates the closest fit to the observed distortion. On the second step, that quad is paired with every

other to find the optimum twofold fit, and so on. This algorithm creates a considerable amount of numerical work and is thereby limited for our most readily available computer⁽⁵⁾ to about twelve-fold fits. The spatial resolution of the $\Delta B/B_0$ plot from Eq. (7) does not pinpoint single magnets with certainty, but typically this search algorithm makes selections from the middle of the peaks in such a plot, finding the highest peaks first.

Test Cases and Results

The closed-orbit distortion shown in Fig. 3 has standard deviation of .6" and maximum of 1"; it is a test case generated by the displacement of all ring quads by random amounts with standard deviation .01". A 12-quad correction was calculated for these data and the same data with .3" standard deviation of random noise added in. For both the perfect and noisy data, the calculation was made for both the data and its 27th-order Fourier sum. The effect of the calculated moves in reducing the true orbit distortion is given in the following table. One sees in this example useful correction when the rms noise is comparable to the rms orbit distortion; the elimination of higher harmonics in the data improves the calculated corrections slightly.

Some real data and its 27th-order sum are shown in Fig. 4. Here at least one detector (indicated by †) is faulty and is ignored. The orbit corrected by the moves of 10 quads (positions marked by X) is shown in the lower curve. This quadrupole set was derived from 12 quads chosen by the search program by substituting for certain moves which were too large. Nearby focusing

magnets were used in place of a defocusing one and the necessary adjustments to the rest of the moves was calculated. With the bad detector ignored, original data and Fourier sum give practically identical results. The plot of $\beta^{3/2} \Delta B / B_0$ is given as Fig. 5 with the chosen quad positions again indicated. The measured closed orbit after correction is shown in Fig. 6 along with that calculated from the magnet moves actually delivered by the crew. This close agreement shows that the data are sufficiently accurate to allow substantially better correction to be obtained in further adjustments. We can get better information from our detectors by adjusting the quadrupole excitation to lower v at the time the measurements are taken. Eq. 3 shows that the principal effect is to increase amplitude of the closed orbit distortion for given ΔB .

The experience of the last year can be summarized by saying that in five sets of moves involving a total of 36 quadrupoles, we have achieved results similar to the above example. Each time it has been useful to consider the data in detail and experiment with various combinations of the techniques described above. Even so, however, the optimum solution usually has differed little from the results of the search algorithm applied to the raw data. The benefits derived from the alternative calculations are principally the checking of the data, the estimation of the degree of correction attainable in a given correction step, and not least important the increased confidence created by a corroborative calculation that the efforts in moving many quadrupole magnets are not being misdirected.

Notes and References

1. E.D. Courant and H.S. Snyder, *Annals of Physics* 3, 1-48 (1958).
2. G.R. Lambertson and L.J. Laslett, *Proc. V Inst. Conf. on High Energy Acc.*, 26-33 (Frascati, 1965).
3. The harmonic correction of the low field orbit was worked out and implemented by Donald A. Edwards completely independently of the work reported here.
4. B. Autin and P.J. Bryant, *Proc. VIII Int. Conf. on High Energy Accelerators*, 515-520 (CERN, 1971).
5. Digital Equipment Corp. PDP-10 with KA-10 processor and 1 μ sec core.

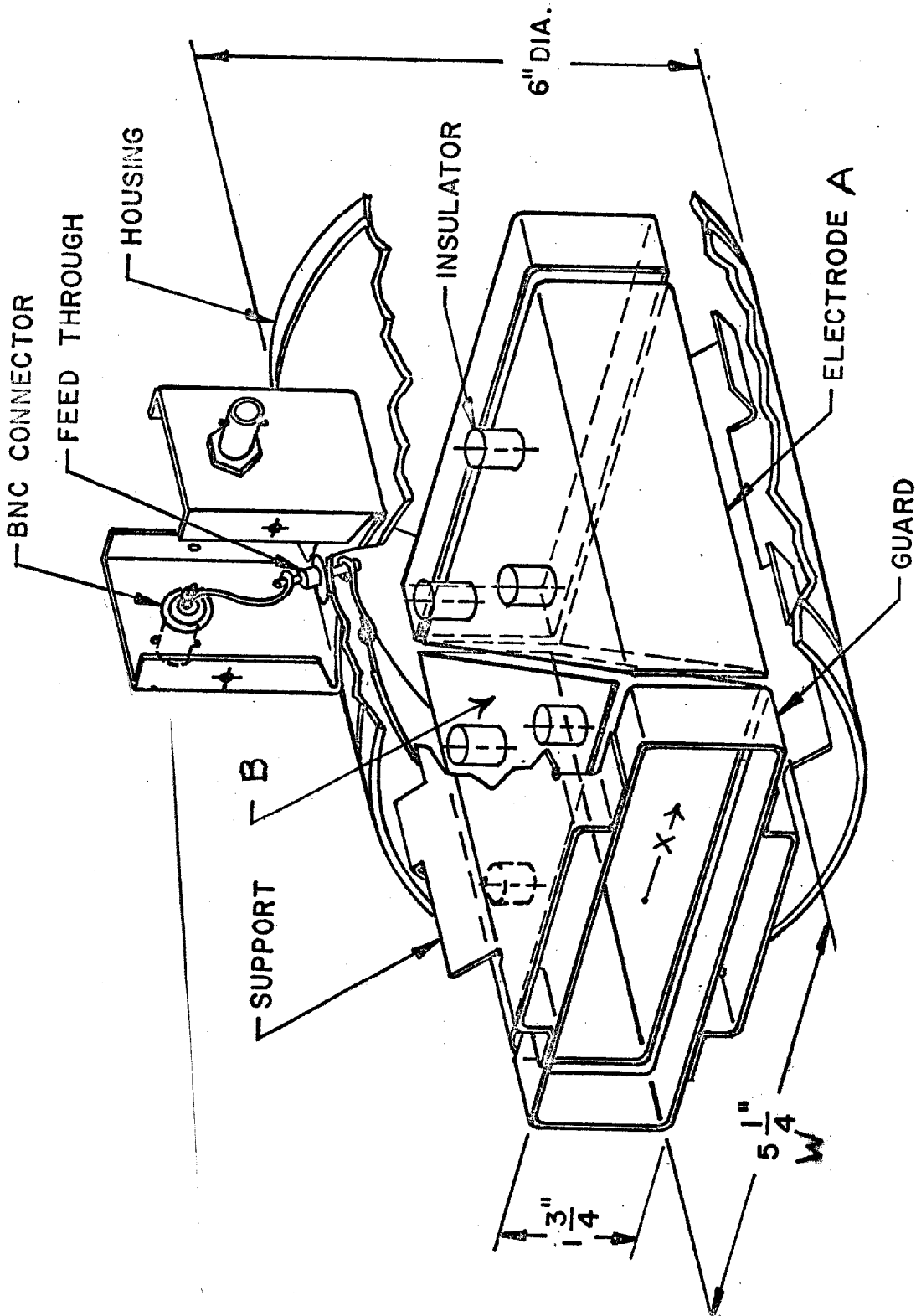
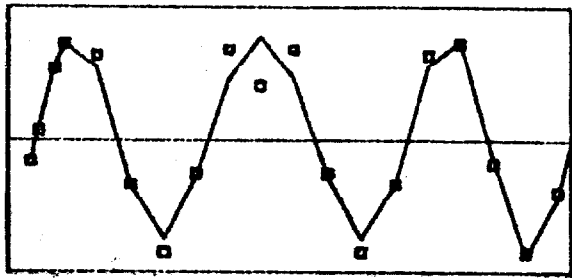
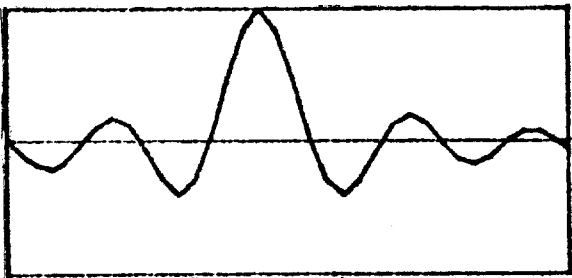


Figure 1 Main ring horizontal beam position detector.

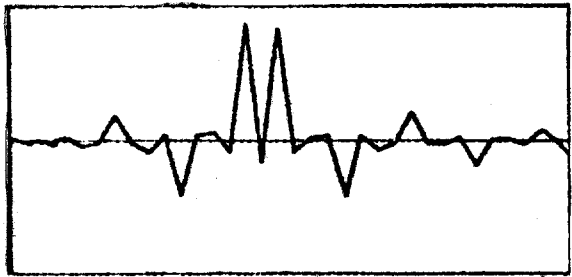


.4 a. Beam sensor readings (\square)
divided by $\beta^{1/2}$ (≈ 10) and
the 27th order Fourier fit.

0
-.4

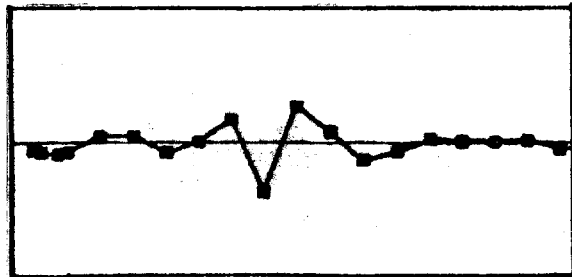


b. $\beta^{-3/2} \Delta B/B_0$ from Fourier fit.



.5" c. Pattern of quadrupole moves.
Largest moves are the
bracketing defocusing quads.

0
-.5"



.4 d. Corrected closed orbit
divided by $\beta^{1/2}$.

0
-.4

Figure 2: Closed-orbit distortion in one superperiod from single focusing quad displaced 1".

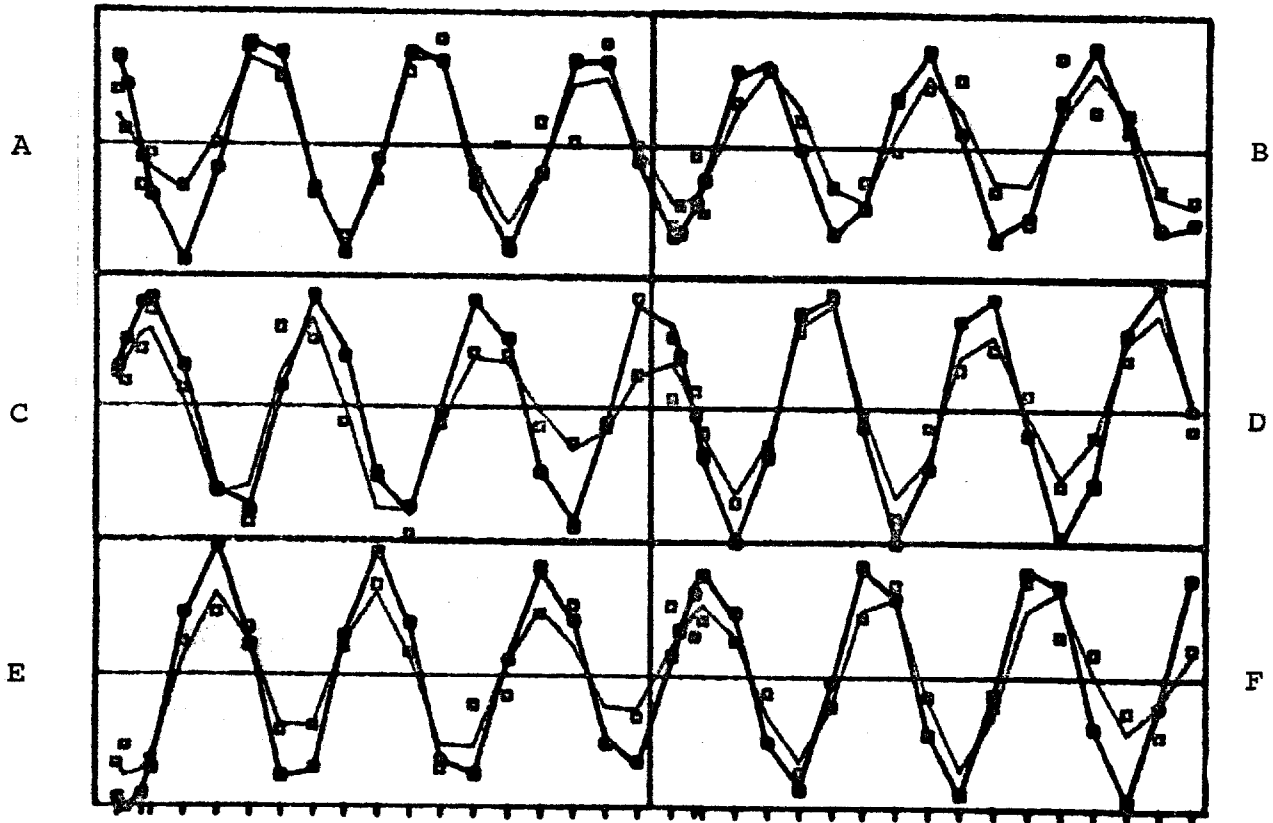
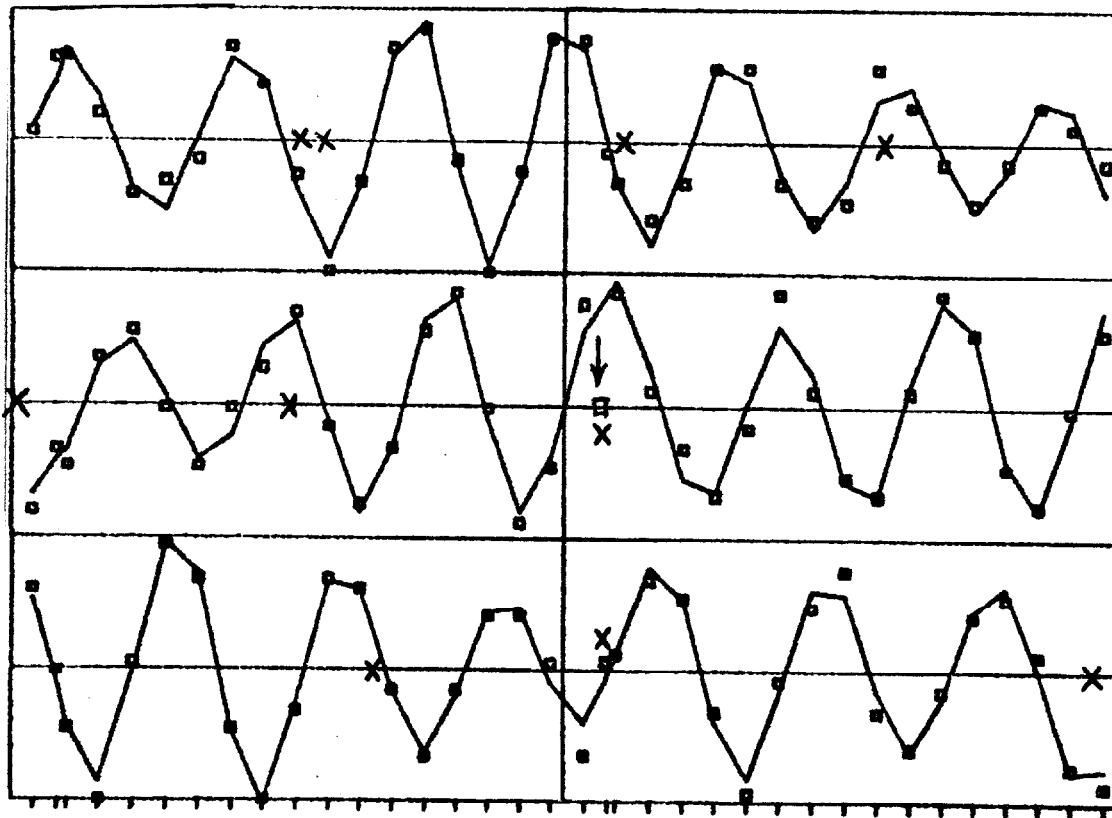
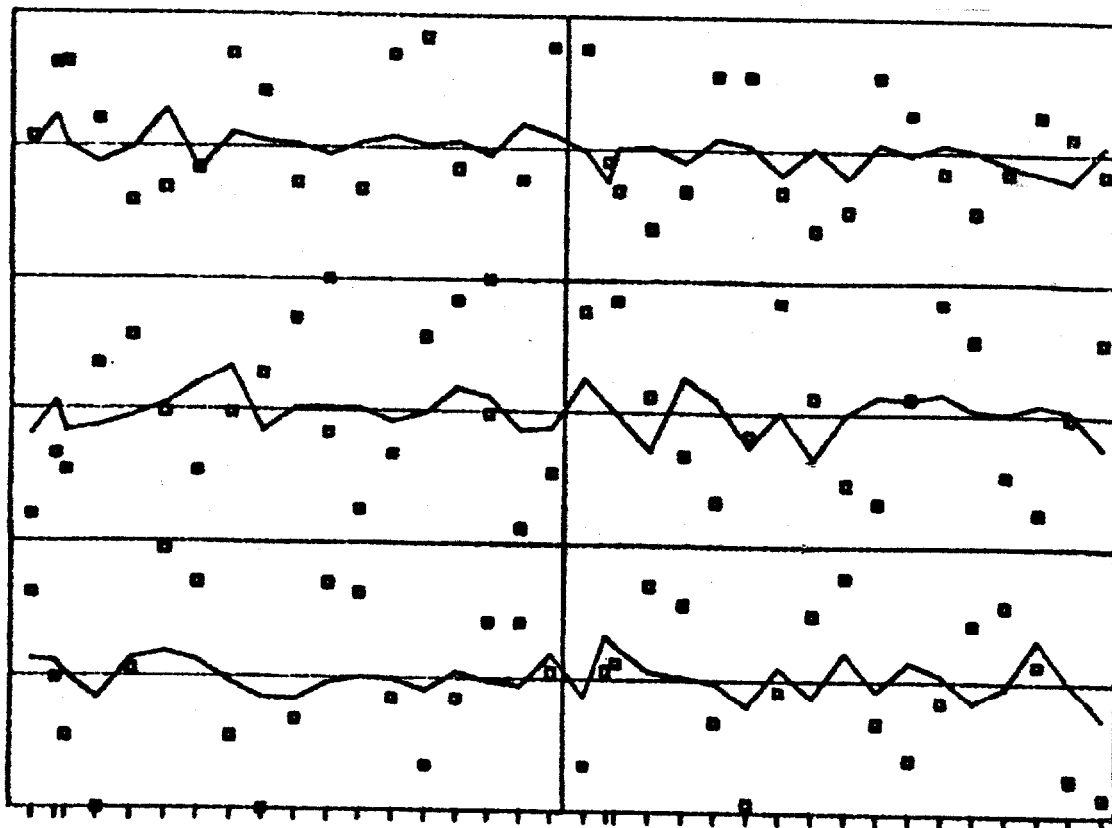


Figure 3: Closed-orbit distortion for the main ring produced by random displacement of quads with $\sigma = .01''$. Scale is $\pm 1''$. The curves are 27th order Fourier fits. The dark curve is without sensor noise; the light curve fits the points with $\sigma = .3''$ of random error added.



(a)



(b)

Figure 4: Vertical closed-orbit distortion (a) measured with 27th-order fit and (b) corrected by ten moves [locations indicated by "X" in (a)].

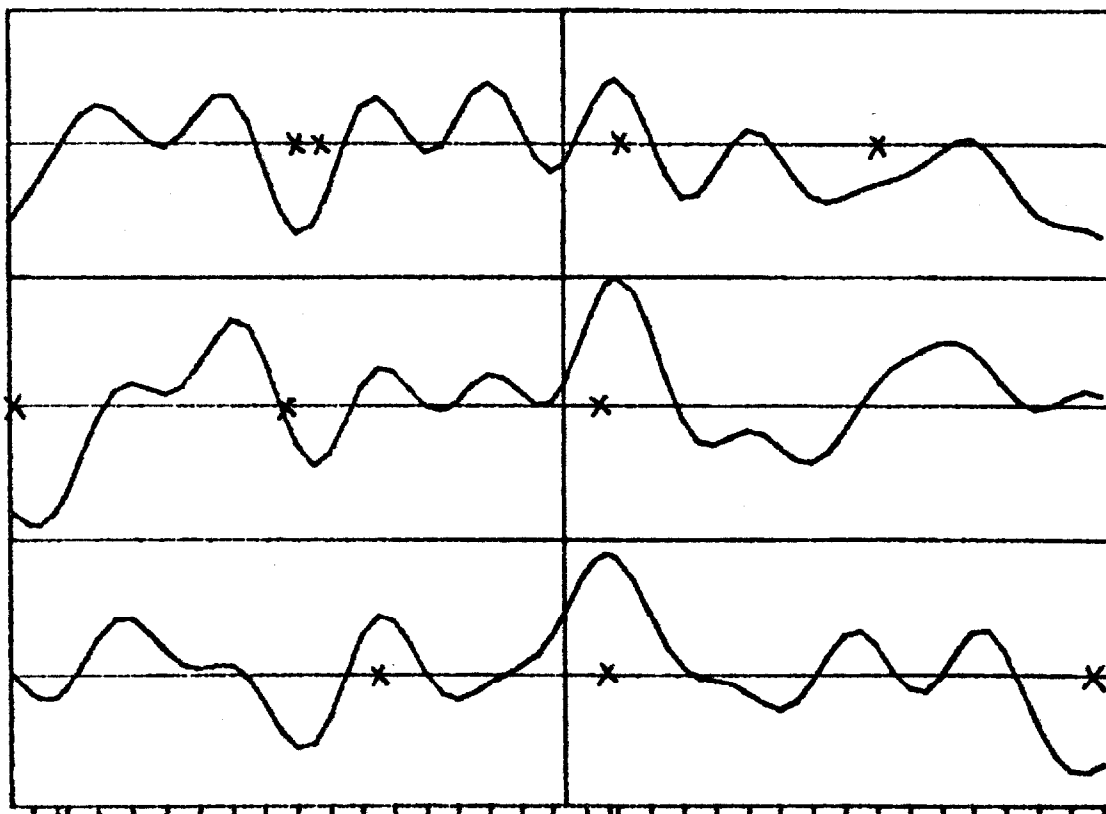


Figure 5: $\beta^{3/2} \Delta B/B_0$ calculated from vertical closed-orbit shown in Fig. 5. Ten quadrupoles chosen to give the corrected orbit shown in Fig. 4 are located at the places marked with "x".

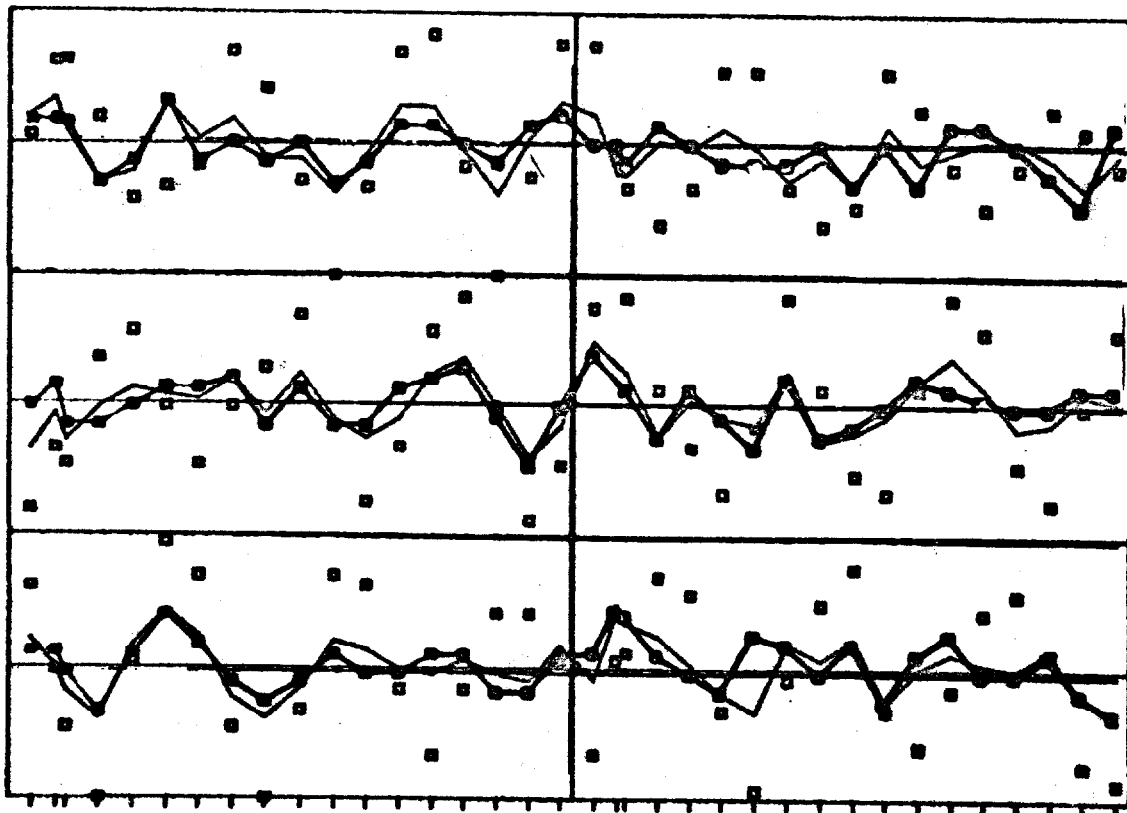


Figure 6: Vertical closed-orbit distortion.
Original detector readings (same as Fig. 4) □ .
Predicted corrected orbit--solid curve.
Measured orbit after correction--curve with
filled boxes.

TABLE

RMS and Maximum Orbit Distortion after 12-Quad Correction

	<u>RMS</u>	<u>Maximum</u>
Before Correction	.59"	1.04"
Perfect Data	.04"	.14"
27th-order Fit to Perfect Data	.05"	.14"
Perfect Data + σ = .3" Random Error	.19"	.62"
27th-order Fit to Data plus Random Error	.17"	.45"